

# DISSOLVED ORGANIC MATTER (DOM) AS NATURAL TRACKING AGENT IN CYCLIC STEAM STIMULATION WITH PREFORMED FOAMS: A MATURE HEAVY OIL FIELD CASE

## MATERIA ORGÁNICA DISUELTA (DOM) COMO AGENTE DE SEGUIMIENTO NATURAL EN ESTIMULACIÓN CÍCLICA POR VAPOR USANDO ESPUMAS PREFORMADAS: UN CASO DE CAMPO DE PETRÓLEO PESADO MADURO

Fernando Andres Rojas-Ruiz<sup>1\*</sup>; Jorge-Armando Orrego-Ruiz<sup>1</sup>; Angela-María Valencia<sup>2</sup>; Romel-Antonio Perez-Romero<sup>1</sup>; Eduardo-José Manrique-Ventura<sup>1</sup>.

### ABSTRACT

The object of this paper was to analyze the non-volatile water-soluble fraction or dissolved organic matter (DOM) from production water associated with Cyclic Steam Stimulation (CSS) with preformed foams through high and ultra-high mass spectrometry. Using ESI FT-ICR MS, six naphthenic acids were identified and selected as new potential natural tracking agents. Subsequently, the DOM fractions were analyzed via ESI MSMS, through which semi-quantitative concentrations of these compounds were established for the samples. The results show that the DOM concentration monitored through ESI-MSMS allows for the correlation of changes during the cycles of steam+foam injection with the increases/decreases of oil production in three wells from the Cocorná Field, Colombia. This information becomes relevant for quality control of cyclic steam injection and, hence, for developing heavy oil mature fields. Thus, monitoring water-soluble petroleum compounds is presented as an affordable strategy and a promising tool to track changes in reservoirs subjected to water injection.

### RESUMEN

En el presente trabajo se analizó la fracción soluble no volátil en agua o materia orgánica disuelta (DOM) obtenida del agua de producción asociada a la Estimulación Cíclica por Vapor (CSS) con espumas preformadas mediante espectrometría de masas de alta y ultra-alta. Utilizando ESI FT-ICR MS, se identificaron y seleccionaron seis ácidos nafténicos como nuevos posibles agentes de seguimiento naturales. Posteriormente, las fracciones de DOM se analizaron mediante ESI MSMS, y se establecieron concentraciones semicuantitativas de estos compuestos para las muestras. Los resultados muestran que la concentración de DOM monitoreada a través de ESI-MSMS permite correlacionar los cambios durante los ciclos de inyección de vapor+espuma con los aumentos/disminuciones de la producción de petróleo en tres pozos del Campo Cocorná, Colombia. Esta información se vuelve relevante para el control de calidad de la inyección cíclica de vapor y, por tanto, para el desarrollo de campos maduros de petróleo pesado.

De esta manera, monitorear compuestos de petróleo solubles en agua se presenta como una estrategia asequible y una herramienta prometedora para seguir cambios en yacimientos sometidos a inyección de agua.

### KEYWORDS / PALABRAS CLAVE

Dissolved organic matter | Preformed Foams | Cyclic Steam Stimulation | Enhanced Oil Recovery  
Materia orgánica disuelta | Espumas Preformadas | Estimulación cíclica de vapor | Recuperación mejorada de petróleo.

### AFFILIATION

<sup>1</sup>Ecopetrol S.A. – Instituto Colombiano del Petróleo y energías de la Transición ICPET Piedecuesta, Santander-Colombia.  
<sup>2</sup>PSL Proanálisis SAS Floridablanca-Santander-Colombia  
\*email: fernandoa.rojas@ecopetrol.com.co

## 1. INTRODUCTION

Steam injection is a thermal Enhanced Oil Recovery (EOR) technology to develop heavy and extra heavy crude oil reservoirs worldwide. However, oil price volatility, trends in energy transition, and steam injection carbon footprint are factors limiting the commercial deployment of such technology. In response to these new challenges, hybrid steam methods such as cyclic steam stimulation (CSS) with preformed foam have become an energy and environmentally efficient technology for revitalizing mature wells in Colombia. Since mid-2019, six field tests of preformed foam injection before the steam cycle have been implemented. The objective is to generate divergence in the steam injection to contact unswept zones with high oil saturation, allowing the optimization of the CSS processes in mature wells (> 10 cycles) of a heavy oil field located in the Middle Magdalena Valley (MMV), Colombia (Perez et al., 2020). This technology includes injecting the foaming agent (FA) with nitrogen as non-condensable gas using a specially designed wellhead mixer to generate a stable foam at the surface and inject it as a diverting agent before the steam cycle is injected (Pérez et al., 2022).

Since waterflooding is mainly considered a physical process, minimal attention is paid to the detailed chemistry of production water before and during field applications (Yildiz H.O., 1996). Water injection studies have tried to characterize inorganic water-soluble species and their effects, ignoring the content and nature of organic species soluble in water. Despite the generally non-polar nature of oil, some heteroatoms containing compounds exhibit considerable solubility in water (Reyes & Crisosto, 2016; Stanford, L.A., Kim, S., Klein, G.C., Smith, D.F., Rodgers, R.P. and Marshall, 2007). Characterizing such crude oil fraction, known as dissolved organic matter (DOM), becomes important for the oil industry since its composition is closely related to environmental consequences (Derenne & Nguyen, 2014; Reyes & Crisosto, 2016; Liu & Kujawinski, 2015). Recently, research has proven the toxicity of unresolved polar compounds from field-weathered oils (Sørensen et al., 2024), and the weathering of polar/nonpolar petroleum components along an oil spill (Ajaero et al., 2024). At the same time, this composition holds outstanding information for geochemical studies, production allocation, and

reservoir engineering (Gonsior et al., 2011). DOM is an unresolved crude oil fraction comprising various chemicals, including naphthenic acids (NAPS) (Gonsior 2011). It is well known that about 3%wt of some crude oils may correspond to acidic species, where NAPS are highly abundant (Jones et al., 2001; Rudzinski et al., 2002). Conventional DOM analyses include oxygen demand tests (DQO), elemental composition (EA), and different spectrophotometric properties (Leenheer & Croué., 2003). Gas chromatography coupled to mass spectrometry (GC-MS), rapid liquid chromatography-tandem mass spectrometry (Shang et al., 2013), and more recently, Fourier transform ion cyclotron resonance mass spectrometry (FT-ICR MS) coupled to low-voltage electrospray ionization (ESI) have proven to be useful to provide detailed compositional information on volatile fractions (low molecular weight compounds) and non-volatile fractions (high molecular weight compounds) of soil/water (Brown & Rice, 2000; Hatcher et al., 2001) and petroleum, (Aeppli et al., 2012) including DOM (Gonsior 2011; Leenheer & Croué, 2003; Stanford et al., 2007) However, despite works focused specifically on naphthenic acids (Bertheussen et al., 2018; Hindle et al., 2013), little has been explored on developing quantitative methodologies for species present in DOM and their application in industrial processes. For instance, the study on EOR associated water composition from Low Salinity (SmartWater) waterflooding (Villabona-Estupiñan, 2020), and, more recently, the development of chemical treatments to decrease water soluble organic (WSO) content from produced water discharge (Venancio et al., 2024), and approaches related to inter-well tracers tests for reservoir conditions mapping (Maddinelli et al., 2022).

In this work, the non-volatile water-soluble fraction obtained from production water associated with preformed foams CSS processes was analyzed through high and ultra-high mass spectrometry. Using ESI FT-ICR MS, six naphthenic acids were identified and selected as potential natural tracking compounds. Subsequently, the DOM fractions were analyzed via ESI-MSMS, through which semi-quantitative concentrations of these compounds were established for the different waters analyzed.

## 2 EXPERIMENTAL DEVELOPMENT

### MATERIALS AND METHODS

Three wells, Well-A, Well-B, and Well-C were monitored for seven, ten, and six months, respectively. One sample was obtained each month for monitoring the Cyclic Steam Stimulation. That way, considering the time-zero sample at each well, a total of twenty-six water samples were used in this study. Samples were collected in a wellhead separator using plastic 5.0 L containers and consisted of oil and water mixtures. No further treatment was performed over these samples, avoiding any possible alteration of the oil properties and composition, except for the gas released during sampling at atmospheric pressure. Average temperature and pressure conditions during sampling were 70 °C and 700 psi, respectively.

### RESERVOIR/FIELD OVERVIEW

The Corcorná oil field was discovered in 1963, and has been producing under CSS since the early 1980s. All the wells in the field produce from three main sands (A, B, and C) separated by

interbedded shales of the Mugrosa Formation, with spacing of more than 1 Km from each other. Producing sands in all wells show high variability in thickness within the field and high permeability contrast. The latter explains the differences in oil production response under cyclic steam stimulation observed during the field's development plan. Table 1 summarizes the field's basic reservoir and fluid properties (Perez et al., 2020; Pérez et al., 2022; Sequera-Dalton et al., 2024)

**Table 1.** Average reservoir and fluid properties of the sands of interest.

Porosity Range (%)	23-28
Permeability Range (mD)	5-5,000
Depth (ft)	850-1,320
Initial Reservoir Pressure (psi)	948
Initial Reservoir Temperature (°F)	105
Oil Gravity, SC, (°API)	11.5
Oil Viscosity SC, cP	44,475
Formation Brine TDS (ppm)	21,000-25,000

The maturity of the CSS represents an inefficient recovery process as time progresses, and the productivity decrease over time can be explained by high permeability contrasts within the pay (open hole) zones, suggesting that most steam cycles have drained the units with the highest permeability or flow capacity intervals. Therefore, the injection of preformed foams as a conformance strategy was justified.

Figure 1 (Pérez et al., 2022) is a simplified scheme describing the bases that support the use of DOM as possible tracking compounds and thus infer the efficiency of the CSS + Foams. Steam injection inefficiency is due to the high permeability contrast along the production zone (left panel). Hence, the preformed foam injection is expected to block the interval with high permeability zone drained during previous cycles and, thus, diverting the steam injected and stimulating the unswept zone (right panel).

As shown in Figure 1 (left), in high permeability zones, the DOM concentrations would tend to decrease as the number of steam cycles increases and oil production decreases (baseline). When the conformance treatment with foam is implemented (Fig. 1, right), the injected steam would stimulate the unswept (lower permeability) zone. Thus, an increase in DOM would be expected due to high oil saturation. At the same time, the foaming agent (surfactant) could also be identified and used to support pilot interpretation.

The historical production of the three wells selected for this study show clear differences in the injection and production performance due to lateral and vertical reservoir heterogeneities. These wells

produced between 3 to 20 barrels of oil per day (BOPD) for CSS effect. The foam injection protocol was the same for all wells except the volume of surfactant (foam) injected (3-5 tons) (Pérez et al., 2022). Foam injection varies due to the differences in the thief zone flow capacities. The treatments were suspended at wellhead injection pressures of approximately 100 psi below the safety limit for operations (1,200 psi). After the foam treatment, the steam cycle injected 8,100 bbls of cold-water equivalent using 60-70% steam quality, and injection temperatures of 500-530°F. Soaking time of 5 to 7 days was applied. It is worth mentioning that steam injection rates post-foam injection varied depending on the injectivity of the low permeability intervals of each of the wells.

Production response also was well specific, showing an oil production response between 2 and 3 months after the treatment and peak of production ranging from 40 to 130 BOPD (R. A. Perez et al., 2023). On average, steam cycles performance was extended between 6 to 12 months, maintaining similar operating conditions to previous steam cycles (Pérez et al., 2022). Further details of this project from the design, lab, and engineering studies, pilot implementation and expansion, project economics, and future work have been well documented in the literature (Osma et al., 2019; Perez et al., 2020; Pérez et al., 2022; Perez et al., 2023; Perez-Romero et al., 2020)

Finally and regarding the main scope of this study, the monitoring plan depended on the starting date of the CSS + foam. However, the pandemic limited the full monitoring and well-service program scheduled. Nevertheless, the number of samples analyzed was representative enough to validate the method to monitor steam injection processes.

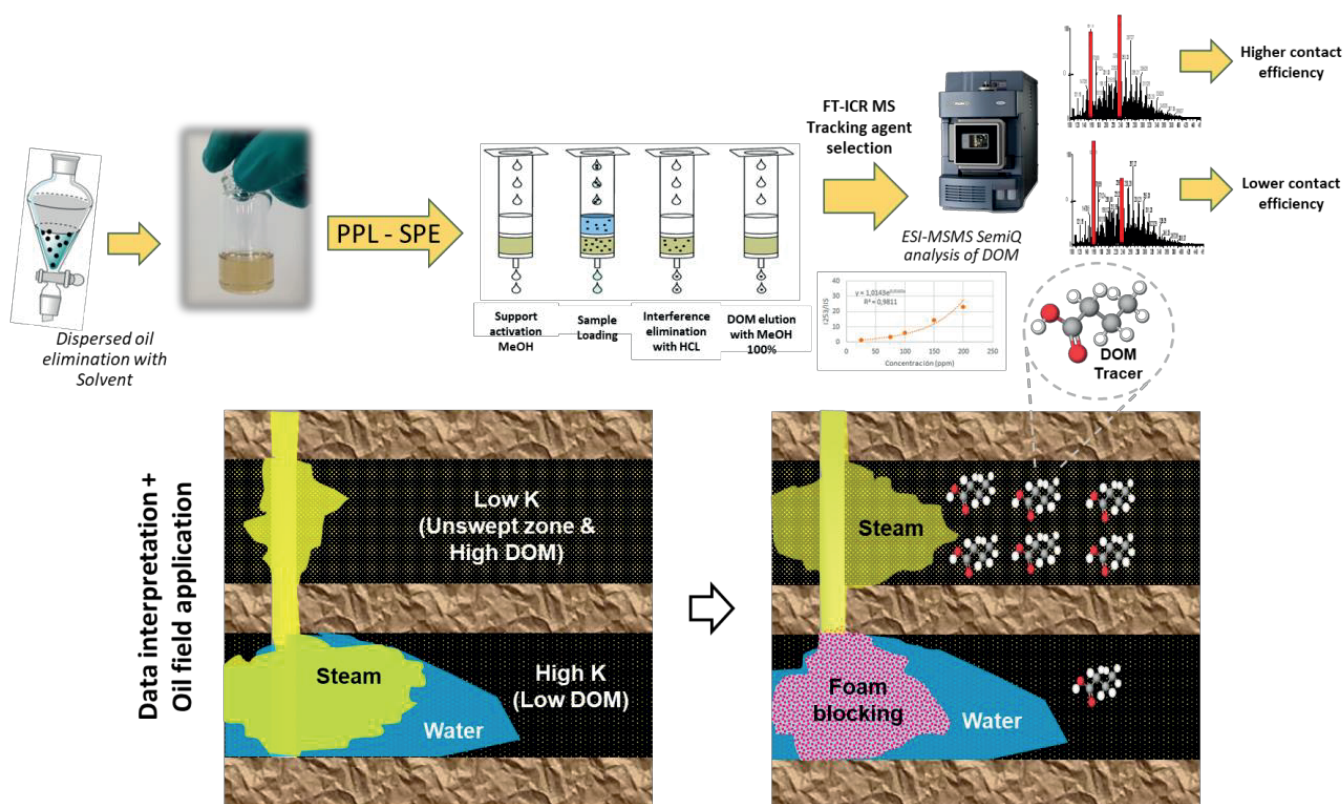


**Figure 1.** Schematic representation of DOM extraction-analysis procedure, and steam stimulation in a high permeability contrast pay zone (left) and after foam blocking of highly depleted steam stimulated interval (right).

## DISSOLVED ORGANIC MATTER (DOM) EXTRACTION

Liquid-Liquid (LL) extraction of DOM was performed as follows, based on the results reported by Zito et al. (Zito et al., 2019): One liter (1L) of production water was obtained by draining the production fluid and filtering using a 42- $\mu\text{m}$  membrane (Whatman 42 paper). Next, a liquid-liquid extraction process was carried out using a 1:1 ratio with n-hexane, to eliminate residual crude oil from the extracted water. Once the extraction with n-hexane was conducted, the pH was adjusted using 0.01 mol/L HCl to favor the protonated acid species in the water phase for their subsequent extraction with dichloromethane (DCM). DCM extraction was carried out using a 1:2 ratio, sample:DCM. The extraction process was performed at a total volume of 500 mL of sample (4 x 125 mL), extracted in duplicate with the same volume of DCM. The extracts were concentrated in vacuo using a rotary evaporator.

Solid phase extraction (SPE) of DOM was performed as follows: One liter (1L) of production water was obtained by draining the production fluid and then filtered using a 42  $\mu\text{m}$  membrane (Whatman 42). Next, to eliminate residual crude oil from the filtered water, a liquid-liquid extraction process was carried out using a 1:1 water to n-hexane ratio for 250 mL of sample. After n-hexane extraction, the 250 mL of production water were acidified with 0.01 mol/L HCl to pH 2. Then, the solid phase extraction process was carried out using a PPL (Priority PolLutant) cartridge, a polymer modified styrene-divinylbenzene from Agilent® Bondelute, previously activated with 60 mL of methanol. After activation, 250 mL of the previously extracted sample with n-hexane were loaded. Subsequently, the water fraction was washed using 2 volumes of 0.01 mol/L HCl to eliminate interferences, mainly inorganic salts. The cartridge was completely air-dried, and the extract (DOM) was eluted with two volumes of MeOH (Dittmar et al., 2008). The extract was collected in a flat-bottom flask and rota-evaporated to dryness to remove water traces. The extract was reconstituted in DCM and transferred to a pre-weighed vial. The final mass was recorded to determine the DOM content for each water sample. Experiments regarding the partition coefficients between oil and water for DOM compounds are off the scope of this work, as well as how these compounds are affected by depressurization and temperature gradients along the production lines.

## CHARACTERIZATION OF SAMPLES VIA (-) ESI FT ICR MS

DOM fractions were analyzed throughout Fourier transform ion cyclotron resonance mass spectrometry (FT-ICR MS) using negative Electro-Spray Ionization (ESI). These analyses were performed using a Bruker Solarix FT-ICR mass spectrometer equipped with an actively shielded 15 T superconducting magnet. DOM extracts were re-dissolved in methanol acetonitrile (50:50) to approximately 10 mg/mL for (-) ESI spectra acquisitions and diluted to 0.005 mg/mL toluene:methanol (20:80). 1.0 % (V/V) ammonium hydroxide was spiked before sample injection. Samples were infused at a flow rate of 150  $\mu\text{L}/\text{h}$  using a syringe pump via an Apollo II electrospray source. Source optics were operated with -20 V for the capillary column end and -50 V for skimmer1 voltages. Ions were accumulated for 0.050 s in a collision cell with 5 MHz frequency and 350 Vpp of radiofrequency (rf) amplitude. The optimized mass for Q1 was 200 Da. The collision cell was operated at 2 MHz and 1400Vpp of rf amplitude. The time-of-flight (TOF) was set to 0.7 ms to transfer the ions to an ICR cell by an electrostatic focusing ion guide operating at 4 MHz and 350 Vpp of rf amplitude. A 150–1000 Da mass range and 4 M acquired data size were used. The time domain data sets

were co-added from 100 data acquisitions. The mass spectra were calibrated internally using Data Analysis (Bruker Daltonics) with an homologous series from  $\text{O}_2$  class DBE 3, using relatively abundant peaks greater than 5 times the signal-to-noise ratio. Elemental composition assignment for each peak was performed using Composer 64 software version 1.5.6 (Sierra Analytics) after exporting the data to a spreadsheet.

## CHARACTERIZATION OF SAMPLES BY ELECTROSPRAY ESI-MSMS

Mass spectrometry analyses were performed on a Waters® XEVO® triple quadrupole detector (TQD) mass spectrometer equipped with a tandem quadrupole mass detector designed for high-throughput LC-MS/MS applications, with the mass analyzer's T-Wave mechanism providing MRM (Multiple Reaction Monitoring) mode analysis. Prepared solutions were injected through the infusion port at a 20  $\mu\text{L}/\text{min}$  flow rate. The ionization conditions were established as follows: capillary voltage 1.4 kV, Cone voltage 30 V, collision energy 20 V, source temperature 120°C, desolvation temperature 600°C, desolvation gas flow rate 800L/hr, resolution (1) LM (low mass) and HM (high mass) 10 and 14.1 respectively; ion energy (1) 0.2, resolution (2) LM and HM 10.5 and 20.1 respectively and ion energy (2) 0.8. Nitrogen (>99% purity) and argon (99% purity) were used as nebulization and collision gases (product ion scanning MS/MS), respectively. Data acquisition was performed in MCA format (multi-channel acquisition), in a mass-to-charge ratio range of 120 -1000 m/z, with an acquisition time of 3 min, each scan time of 10 s, utilizing the Mass Lynx™ software. The data of each acquisition was exported to Excel to be processed. The evaluation of the potential interference of the individual crude oil ionized species with the solvent signals, the solvent (methanol/toluene 90:10 with the addition of 2-fluorobenzoic acid (2-FBA) as standard) mass spectrum peaks was performed. Therefore, any possible interference was ruled out when analyzing the sample's mass spectra in the presence of solvent and the 2-FBA.

# 3. RESULTS & ANALYSIS

## OBTAINING DISSOLVED ORGANIC MATTER (DOM)

Baseline (BL) water samples from Well-A BL, Well-B BL, and Well-C BL were extracted in duplicate throughout LL and SPE procedures, and the results displayed in Figure 2 are the average percentage of DOM in water. Raw data regarding this observation is presented as individual data sets in supporting information (Table S1). In general, the percentage of dissolved organic matter did not exceed 0.015% in all cases, and it was not below 0.0035%. When comparing the two methods, it can be said that the SPE provided a higher percentage of DOM extraction than the LL method. Based on these results, and in agreement with literature (Gonsior, 2011; Zheng et al., 2020; Zito et al., 2019) SPE extraction was chosen for further DOM extraction with monitoring purposes.

## CHARACTERIZATION OF SAMPLES VIA (-) ESI FT ICR MS

The relative abundance of the compounds detected by (-) ESI FT-ICR MS is presented in Figure 3, which provides information on the chemical nature of the compounds present in DOM extracts. For better understanding of the results, the classes were sorted as Oxy-nitrogenous (NOX, with x=1 to 5), sodium adducts ( $\text{NaO}_3$ ,

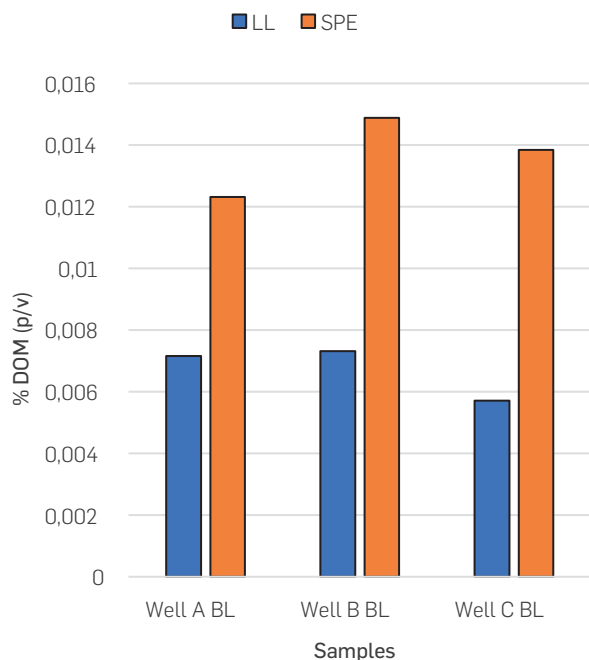


**Figure 2.** Liquid-liquid (LL) vs. solid phase (SPE) extraction comparison.

NaO<sub>3</sub>S, NaO<sub>4</sub> and NaOS), oxygenated (Ox, with x=1 to 6), and oxy-sulfured (OxS, with x=1 to 5) families, summing the respective abundances in each case, as shown in Figure 3b. Figure 3a shows the relative abundance of all classes detected for three BL samples, i.e., the composition before the steam-foam treatment. According to these data, DOM is mainly composed of highly polar compounds, as expected, containing one to six oxygen atoms per molecule.

The most abundant class was O<sub>4</sub>, accounting for more than 35 % RA in all cases, followed by the O<sub>2</sub> class with more than 10 % RA. Regarding such families, the most abundant classes were NO<sub>3</sub> for oxy-nitrogenous, NaO<sub>4</sub> for sodium adducts, O<sub>4</sub> for oxygenated, and O<sub>3</sub>S for oxy-sulfured. On the other hand, the oxygen-containing species were the most abundant family (Ox) in all cases, comprising more than 63 % RA of the relative abundance. Oxy-nitrogenous had an average of 13.4 %, Sodium adducts 10.8 % RA, and oxy-sulfured 9.3 % RA.

Among the oxygenated, the classes O<sub>2</sub>, O<sub>3</sub>, and O<sub>4</sub> were examined in detail since they represent the most abundant oxygen-containing compounds. The double bond equivalent (DBE) distributions for the classes O<sub>2</sub>, O<sub>3</sub>, and O<sub>4</sub> were plotted to obtain additional information regarding the aromaticity/naphthenic systems of the molecules concentrated in the DOM (Figure 4). Class O<sub>2</sub> presents a triple distribution with maximums at DBE 1, 3, and 7, class O<sub>3</sub> presents its maximum around DBE 5 and a shoulder around DBE 7, and class O<sub>4</sub> has a maximum of DBE 4 and a shoulder in DBE 8. Based on the information provided by the FT-ICR-MS, it is possible to state that the main species contained in the DOM and concentrated via solvent extraction are associated with poly-alcoholic compounds (sterol derivatives) or naphthenic acids, according to what was reported previously (Sleighter & Hatcher, 2007; Zheng et al., 2020)

Additionally, the DBE vs. Carbon number contour plots (Figure 5) were assessed to provide a more detailed interpretation. All the compounds in Figure 5 had carbon numbers between C<sub>12</sub> and C<sub>23</sub> and DBE between 3 and 10 (from naphthenic to di-aromatic compounds). Unimodal distributions were detected for classes O<sub>3</sub>, O<sub>4</sub>, NO<sub>3</sub>, and O<sub>3</sub>S. For O<sub>1</sub>, bi-modal distributions for O<sub>1</sub> and O<sub>2</sub> were observed, which encompass DBE 4 to 6 and DBE 7 to 10. From these results, it can be stated that the most abundant compounds, according to each class, had between 15 and 20 carbon numbers and DBE between 4 and 7.

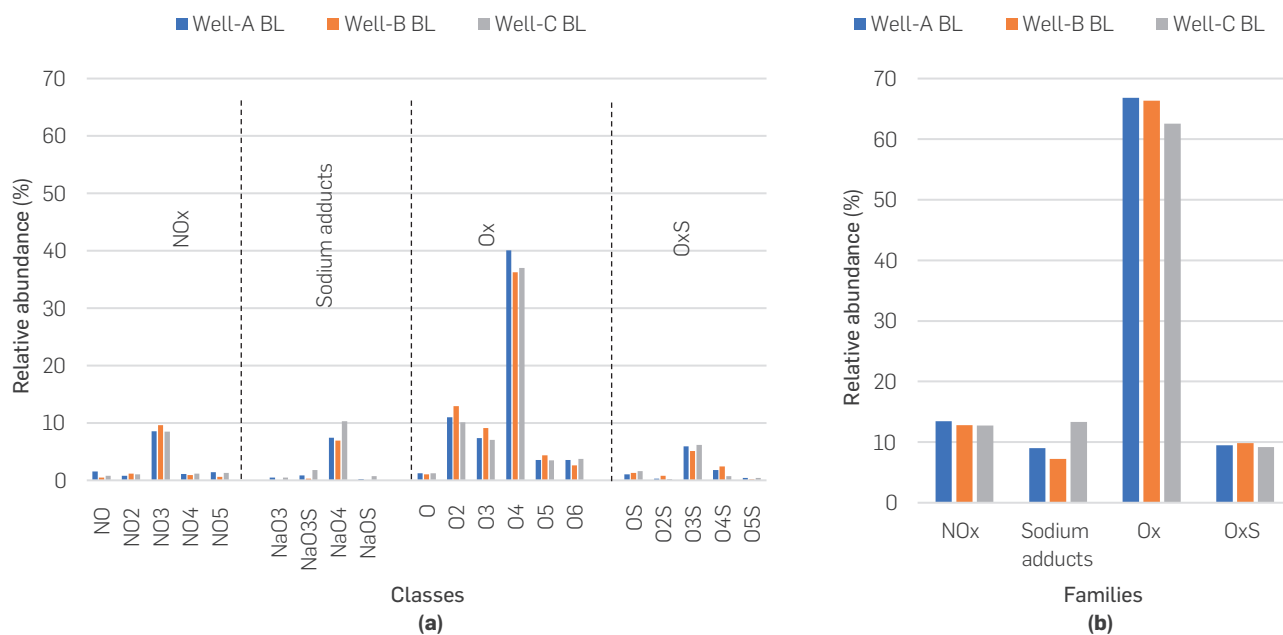


**Figure 3.** Relative abundance of (a) classes detected by (-) ESI FT-ICR-MS and (b) families of compounds in DOM for baseline samples.

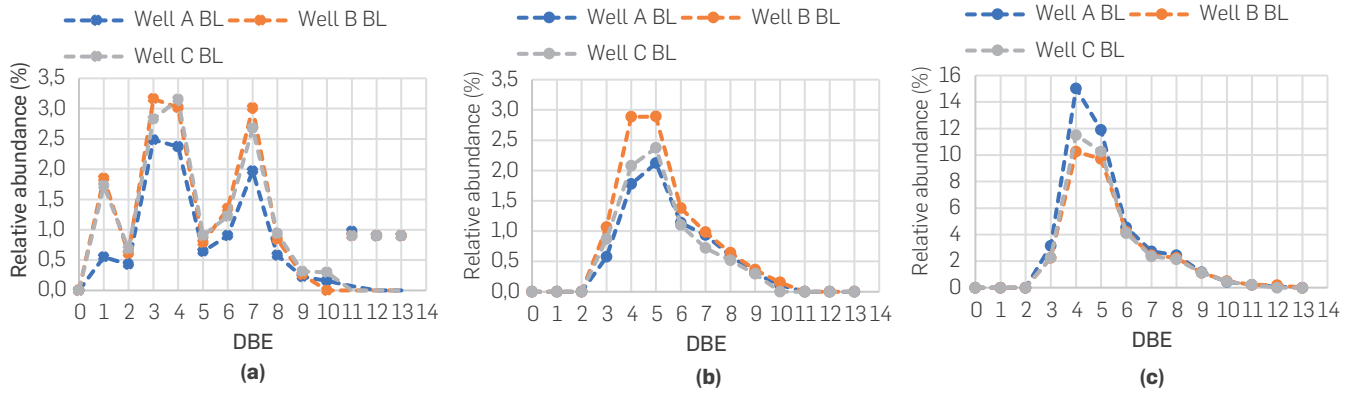


**Figure 4.** DBE distributions for classes (a) O<sub>2</sub>, (b) O<sub>3</sub>, and (c) O<sub>4</sub> in DOM for base line samples.

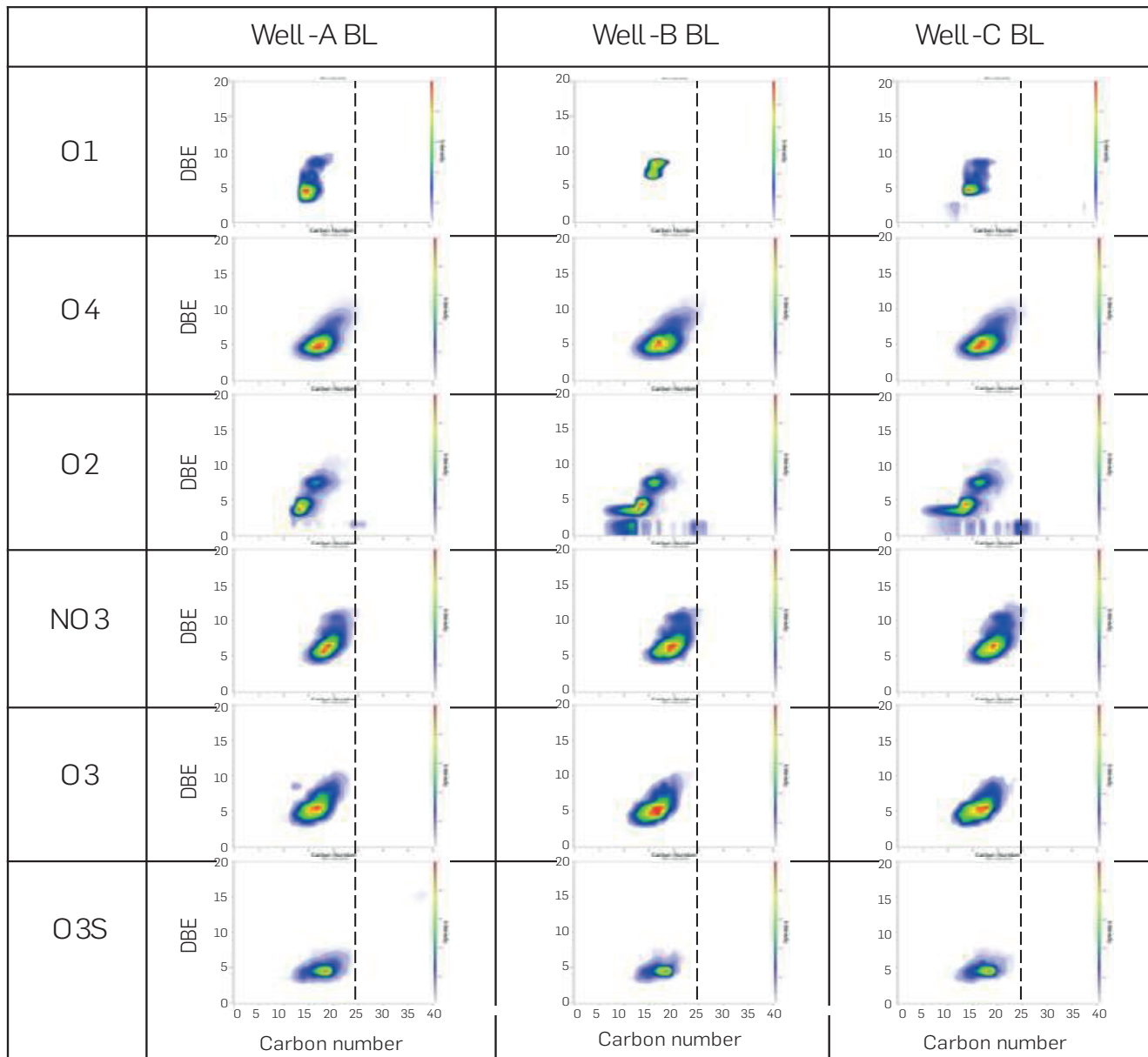


**Figure 5.** DBE vs. CN contour plots for chosen classes.

## SEMI-QUANTITATIVE ESI MSMS ANALYSIS

In parallel, the DOM extracts obtained were analyzed by mass spectrometry ESI MSMS to compare the obtained data and identify the best ions for subsequent quantification. Thus, the ESI MSMS protocol depicted in the experimental section allowed the identification of 6 ions common to all the analyzed water samples whose intensities (relative abundance) were particular for each DOM extract. Then, ESI-MSMS data analysis was crossed with the FT ICR MS results, providing information on the compositional changes of the production water during and after foam injection and, thus, correlating the selected ions as natural tracking compounds in enhanced oil recovery processes. Table 2 presents the comparison of information obtained by each mass spectrometry technique. Based on the literature and considering factors such as m/z ratio, DBE, Class, molecular formula, and the hydrogen deficiency coefficient (Z number), the chemical nature of the assessed natural tracking agents were associated with water-soluble naphthenic acids (McCormack et al., 2001; Rowland et al., 2011; Thomas et al., 2009).

Figure 6 displays the parallel between FT ICR MS and ESI MSMS spectra at a nominal mass of 295 Da. The most abundant species correspond to 295.19683 for ultra-high-resolution spectra with a molecular formula  $C_{17}H_{28}O_4$ . Regarding the ESI-MSMS spectra, the highest abundance corresponds to m/z 295.28, with a difference of 0.09 Da (0.03%) compared to FT ICR MS. Bearing this in mind and to simplify and speed up the monitoring analysis using ESI MSMS, ions detected within 0.01-0.09 Da difference compared to FT ICR MS were assumed as the corresponding naphthenic acids comprised among the most abundant class  $O_4$ , and considered for semiquantitative natural tracking compounds' analysis (see Table 3 for comparison)

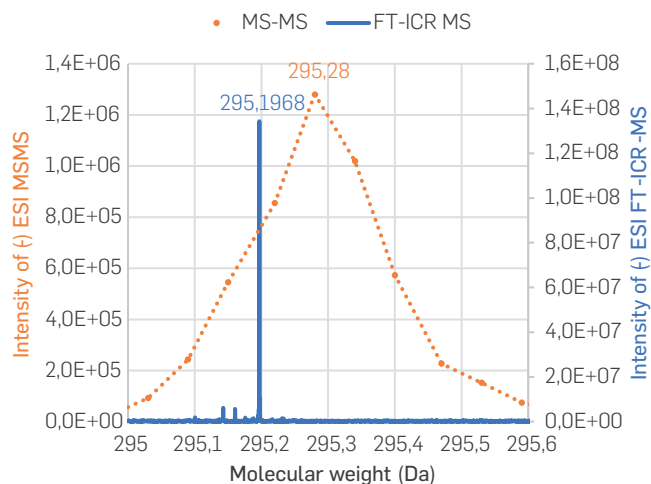


**Figure 6.** FT-ICR MS vs. ESI-MSMS spectra resolution.

For the semi-quantification of the signals, 2-FBA was employed as an internal standard to normalize the signal of the measured samples. The processed samples were infused into the mass detector through an electrospray ionization chamber in negative mode (ESI neg). MS/MS data acquisition was performed under MS scan mode, and mass parameters were optimized according to the chemical nature of the obtained DOM. An equimolar mixture of all the baseline samples was prepared to develop the method and establish a concentration value for each of the m/z ratios proposed as natural tracking species. Such a mixture was labeled as COC BL. Subsequently, mass spectra of COC BL were acquired via ESI-MSMS at 25, 75, 100, 150, and 250 ppm (Figure 7), using the 2-FBA at 25 mg/L as an internal standard.

**Table 2.** Compositional information from FT-ICR-MS and MS/MS

CLASS	FT-ICR MS						ESI-MSMS
	m/z	DBE	Experimental Mass	Formula	Abundance	Z number	ion
$O_4$	309	4	309,2071	$C_{18}H_{30}O_4$	3,02E+08	-6	309,28
$O_3$	309	3	309,2435	$C_{19}H_{34}O_3$	1,61E+06	-4	
$O_2$	309	9	309,186	$C_{21}H_{26}O_2$	3,50E+06	-16	
$O_2S$	309	4	309,1894	$C_{18}H_{30}O_2S$	1,67E+06	-6	
$O_4$	295	4	295,1914	$C_{17}H_{28}O_4$	2,93E+08	-6	295,28
$O_3$	295	3	295,2279	$C_{18}H_{32}O_3$	3,72E+06	-4	
$O_2$	295	9	295,1704	$C_{20}H_{24}O_2$	3,57E+06	-16	
$O_2S$	295	4	295,1737	$C_{17}H_{28}O_2S$	1,67E+06	-6	
$O_4$	281	4	281,1758	$C_{16}H_{26}O_4$	2,82E+08	-6	281,21
$O_3$	281	3	281,2122	$C_{17}H_{30}O_3$	5,13E+06	-4	
$O_2$	281	2	281,2486	$C_{18}H_{34}O_2$	1,12E+07	-2	
$O_2S$	281	4	281,1581	$C_{16}H_{26}O_2S$	1,72E+06	-6	
$O_4$	267	4	267,1602	$C_{15}H_{24}O_4$	1,93E+08	-6	267,21
$O_3$	267	3	267,1966	$C_{16}H_{28}O_3$	9,27E+06	-4	
$O_2$	267	2	267,233	$C_{17}H_{32}O_2$	1,98E+06	-2	
$O_4$	253	4	253,1445	$C_{14}H_{22}O_4$	1,12E+08	-6	253,14 - 253,2
$O_3$	253	3	253,1809	$C_{15}H_{26}O_3$	1,08E+07	-4	
$O_2$	253	2	253,2173	$C_{16}H_{30}O_2$	4,79E+06	-2	
$O_4$	239	4	239,1289	$C_{13}H_{20}O_4$	6,42E+07	-6	239,14 - 239,2
$O_3$	239	3	239,1653	$C_{14}H_{24}O_3$	1,29E+07	-4	
$O_2$	239	2	239,2017	$C_{15}H_{28}O_2$	5,72E+06	-2	

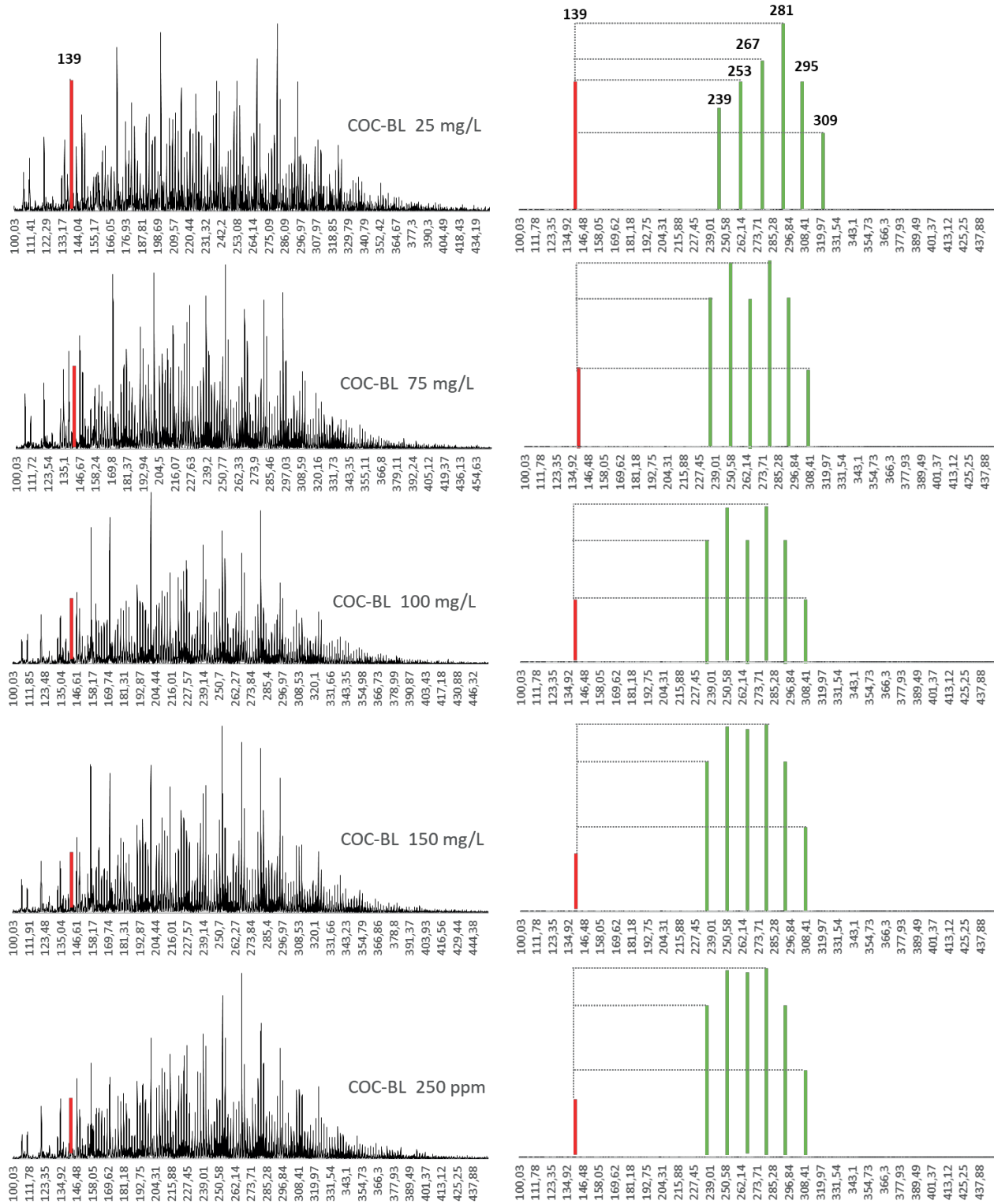


**Figure 7.** ESI-MS/MS spectra for DOM of COC-BL at different concentrations.

As seen in Figure 7, the mass spectra were detected in a mass range of 100 to 450 Da ( $m/z$ ), with variable relative abundance to the  $m/z$  139.11 peak corresponding to the internal standard (2-FBA). For the spectrum obtained at 250 mg/L DOM, the relative abundance of  $m/z$  139.11 was lower, and vice versa for the spectrum at 25 mg/L DOM. Subsequently, peaks at  $m/z$  239, 253, 267, 281, 293, and 309 were chosen to build the calibration curves according to the above analysis (see Table 1). Calibration curves were created using the ratio of the intensity of each tracer chosen over the intensity of the internal standard signal ( $I_{m/z}/I_{IS}$ ), as shown in Figure 8. In all cases, positive non-linear correlations were obtained between the ratio of each peak intensity with the internal standard (2-FBA) and concentration in mg/L. Signal stability and response repeatability was assessed by injecting a reference DOM extract on different times, resulting in a standard deviation range of 0.8 – 1.23 for all the ions studied (see table S3).

On the other hand, once the post-CSS+Foam injection samples were analyzed, differential signals were observed at  $m/z$  293 with respect to COC-BL mass spectra (Figure 9a). These signals were attributed to the foaming agent used (MW 294 Da), according to the supplier's technical specifications regarding its molecular weight and chemical nature (ionic surfactant). Thus, for the  $m/z$  293 ratio, an additional calibration curve was constructed to quantify the corresponding amount of additive present in each sample (Figure 9b).

Thereafter, the concentration of each monitored tracer was calculated for all samples. The final concentration was obtained by averaging the concentration of the six tracking species as DOM. Table 3 summarizes the concentration of these compounds, the DOM concentration for all samples analyzed, and the FA concentration detected. Since no foaming additive was injected/

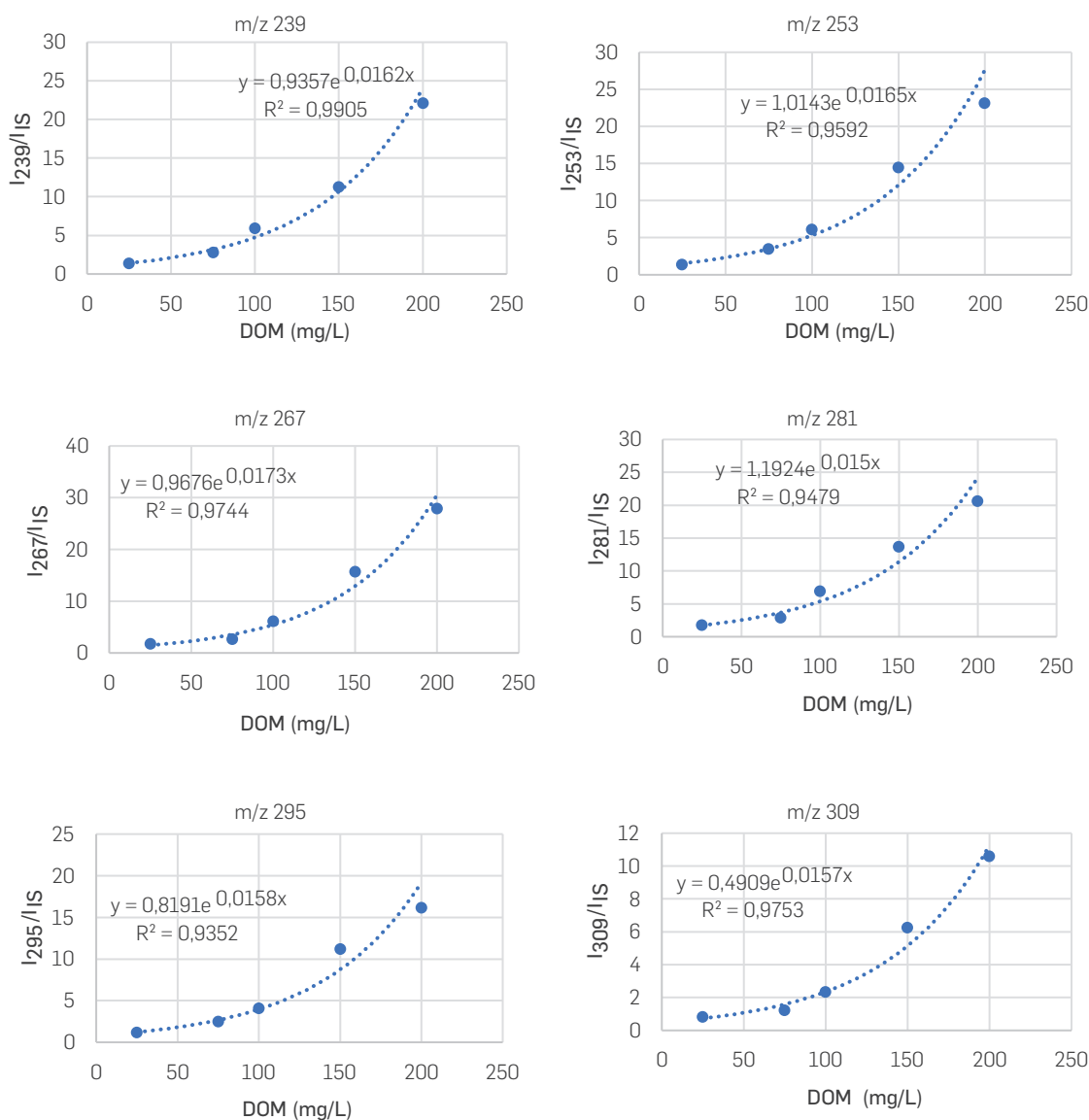


**Figure 8.** Calibration curves for ion ratios selected as natural tracking compounds.

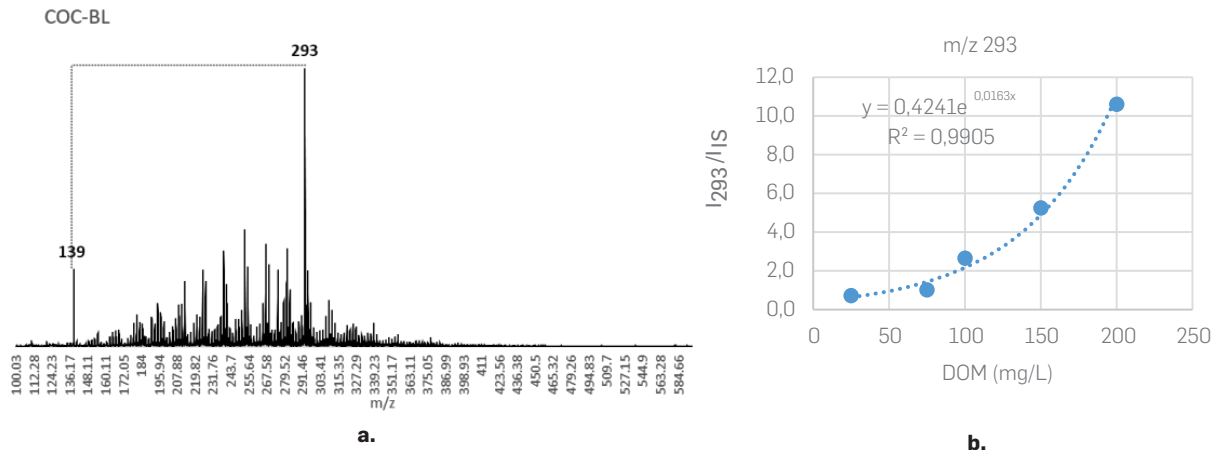


**Figure 9.** a) ESI-MSMS displaying the presence of foam ion m/z 293, b) Foam calibration curve

detected for baseline (BL) samples, an arbitrary quantity (1.0 mg/L) of FA was established for further analytical purposes. Gravimetric data regarding the DOM extractions performed via the SPE-PPL procedure for individual samples are consigned in Table S2.

Figure 10 shows the case of Well-A, where four months after foam injection, the produced oil phase increased from 19 barrels of oil per day (BOPD) to a maximum of 33 BOPD in month 5th (Figure 10, solid line). Water cut during this period decreased by 30 % from its

**Table 3.** Natural tracking compounds dissolved organic matter and foaming agent concentration.

Sample/Month	Natural Tracer m/z (mg/L) & Foaming agent (mg/L)							Average DOM conc. (mg/L)	293 (FA)
	239	253	267	281	295	309			
WELL-A BL	89.7	89.6	93.5	91.1	106.2	98.4	94.7	1.0*	
1	85.3	88.7	95.3	98.5	137.0	112.0	102.8	107.8	
2	92.5	100.0	101.2	101.8	141.2	112.4	108.2	117.5	
3	111.2	114.5	105.9	110.1	154.0	129.9	120.9	146.8	
4	58.9	32.5	37.5	31.6	71.8	43.2	45.9	53.7	
5	63.3	67.9	72.5	63.4	75.0	95.0	72.9	41.9	
6	66.9	74.0	73.0	0	85.2	76.6	62.6	107.1	
7	30.8	37.7	34.6	0	46.5	31.5	30.2	66.6	
WELL-B BL	145.9	150.1	151.3	160.1	159.6	161.1	154.7	1.0*	
1	133.9	138.6	134.8	134.4	199.0	188.3	154.9	374.5	
2	169.7	170.0	165.8	172.4	210.1	199.7	181.3	372.4	
3	184.5	186.9	181.6	186.5	193.7	185.5	186.5	315.8	
4	186.7	194.9	187.0	195.3	186.2	188.2	189.7	266.6	
5	169.6	162.8	157.9	163.6	158.1	160.9	162.2	222.9	
6	195.7	199.8	194.7	206.6	191.3	185.2	195.6	225.2	
7	172.0	176.8	172.4	181.6	166.5	158.3	171.2	185.7	
8	140.1	147.6	145.3	149.8	134.0	122.8	139.9	165.8	
9	62.9	65.8	60.1	0.0	61.9	21.5	45.4	70.6	
10	0.0	34.1	38.1	0.0	42.0	0.0	19.0	39.1	
WELL-C BL	166.9	165.0	158.7	156.9	143.9	128.6	153.4	1.0*	
1	94.0	90.5	91.7	83.7	85.3	84.8	88.3	225.4	
2	264.8	255.6	244.9	247.0	267.9	293.9	262.3	251.3	
3	150.9	142.5	136.0	134.9	127.4	135.4	137.9	181.4	
4	107.2	95.8	96.5	93.1	91.9	94.0	96.4	154.9	
5	200.7	209.0	202.1	217.7	204.6	200.7	205.8	239.6	
6	132.9	135.9	131.9	133.5	123.8	115.8	129.0	162.2	

\*No foaming additive was injected/detected for base line (BL) samples. Thus, an arbitrary quantity (1.0 mg/L) of FA was established with analytical purposes and further data processing.

original value (250 barrels of water per day (BWPD) to 179 BWPD) (Perez et al., 2020). In this case, the concentration of the FA (Figure 10, dashed line) detected is consistent with the concentration of DOM in such water phase (Figure 10, bars). From month 4, the oil production correlated with FA and DOM concentration. As can be seen, there is an increase in DOM from BL until reaching a maximum of 114 mg/L in month 3. The FA concentration and DOM decreased notably for the sample collected in month 4. Curiously, DOM, FA, and oil phase increased again in month 5 and decayed in month 6. Such behavior would mean that the foam blocked the interval after 5 months, mainly drained during previous cycles, and the steam stimulated an unswept zone, increasing the oil production.

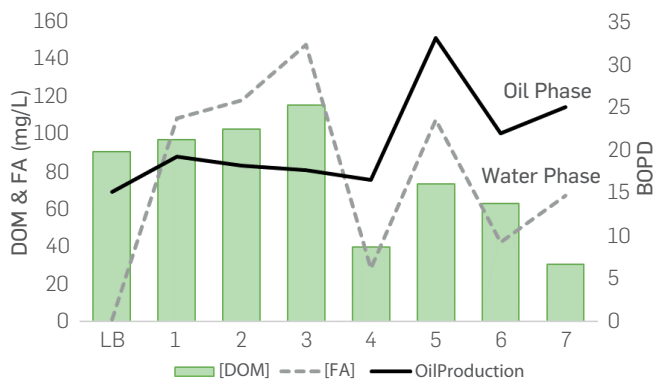


**Figure 10.** Monitoring over the time of the well Well-A during CSS.

Figure 11 represents the case of Well-B, where, in the first month of CSS+foam injection, the oil production increased significantly, from 5 BOPD to 58 BOPD (Figure 11, solid line). The produced water decreased from 250 to 218 BWPD. However, the DOM seemed constant from month 1 to 8 (Figure 11, bars). The foaming agent reached a maximum concentration between months 1 and 2 (28 mg/L) and subsequently its concentration decreased (Figure 11, dashed line). The same trend was observed in the oil production data, where the concentration of the foaming agent matched the decreasing behavior in oil production. From month 1 to month 8, the oil production correlated with foam but not with DOM. The increase in the foaming agent at the early stages of the cycle was expected with high volumes of condensed steam produced. This last result can be attributed to a possible excess of the foam volume injected. However, as the cycle evolved, the foaming agent concentration decreased gradually, suggesting stability. Moreover, such performance explains the oil production rates above the baseline, which were noticed right before implementing the CSS + Foam.

Finally, Figure 12 shows the case of Well-C, where oil production increased upfront in the CSS+foam injection (5 BOPD to 26 BOPD) (Figure 12, solid line) and the DOM concentration grew, reaching its maximum in the water phase (262 mg/L) (Figure 12, bars). Beyond the baseline, DOM increased and reached a maximum concentration after the second month. Comparing these data with oil production, it is observed that once the treatment with the foaming agent started, the oil production increased, reaching a maximum in month 2 (26 BOPD), and later decreasing gradually to around 10 BOPD.

When comparing the behavior of DOM concentration over time concerning the foaming agent concentration (Figure 12, dashed line) and the monthly oil production values, it was noticed that in

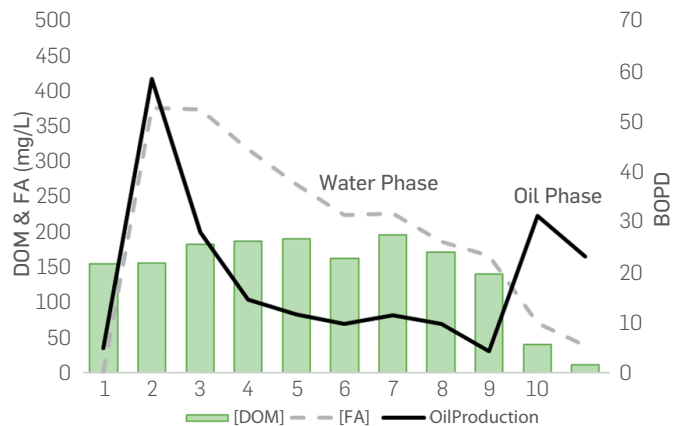


**Figure 11.** Monitoring over the time of the well WELL-B during CSS.

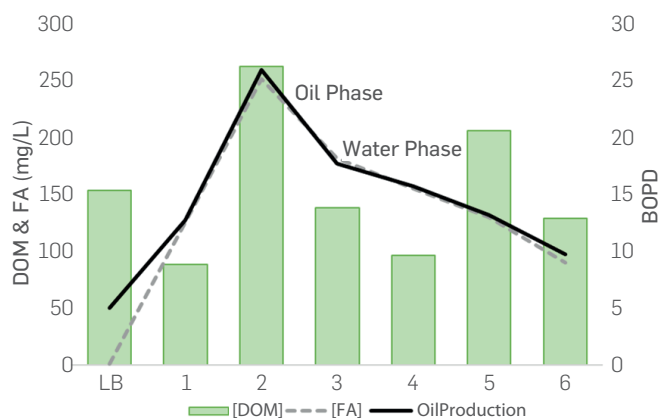


**Figure 12.** Monitoring over the time of the well WELL-C during CSS.

month two, the concentration of DOM increased consistently with the oil production. Subsequently, oil production decreased with the foaming agent and DOM, which concentration decreased to a minimum value in month 4. In this case, it can be inferred that the foam cycle applied in Well C was efficient, favoring the contact of injection water with the residual oil in the unswept zones. Such a result is consistent with the pressure increase response observed at the end of the foam cycle (Perez et al., 2023). Pressure increase helps to infer the blocking effects of the preformed foam in the reservoir (Pérez et al., 2022).

As can be noticed from the results obtained for the three wells studied, there is a positive correlation between the amount of DOM detected in the water produced after the foam-CSS process and the crude oil production (BOPD). Bearing in mind that water washing favors the removal of compounds with high polarity or aqueous solubility and that such compounds are relatively limited within the oil (altering oil composition) (Ghassal, 2019; Wang et al., 2016), these correlations can be understood as a result of additional water washing that is favored by the blocking effect caused by the foam, and that allows the steam contacting fresh crude oil, with higher concentrations of unwashed water-soluble compounds (natural tracking compounds), increasing DOM values as the barrels produced augment.

## CONCLUSIONS

In this work, using commercially available SPE cartridges and feasible experimental methodologies, the dissolved organic matter (DOM) from different Colombian oil wells was extracted for analytical purposes. Based on (-) ESI FT-ICR MS analysis, specific DOM ions were identified and selected as potential natural tracking compounds for preformed foams steam injection performed in the Cocona's oil field. Then, using ESI-MSMS, a semi-quantitative method was developed for DOM concentration monitoring along the foam-steam injection. The increase in the total concentration of DOM indicates the contact of water with oil at unswept zones within the pay interval (residual oil in place) and agrees with the oil production increases (BOPD) observed after the foam-steam injection cycle. This information becomes relevant for the quality control of cyclic steam injection and, hence, for developing heavy oil

mature fields. It also opens the possibility of using natural water-soluble compounds in future non-thermal EOR technologies and reservoir geochemistry. Based on the incremental oil recovery from these pilot wells, hundreds of candidate wells have been identified for continuing the technology development plan, justified by NG savings, the low cost of implementation, and a low breakeven oil price (32 USD/bbl) (Perez et al., 2023).

## ACKNOWLEDGEMENTS

The authors would like to express our gratefulness to Ecopetrol S.A No. 5222395 for allowing the publication of these results and to the Vice-Presidency of Science, Technology & Innovation of Ecopetrol S.A for its technical and financial support.

## REFERENCES

- Aeppli, C., Carmichael, C. A., Nelson, R. K., Lemkau, K. L., Graham, W. M., Redmond, M. C., ... & Reddy, C. M. (2012). Oil weathering after the Deepwater Horizon disaster led to the formation of oxygenated residues. *Environmental science & technology*, 46(16), 8799-8807. <https://doi.org/10.1021/es3015138>
- Ajaero, C., Vander Meulen, I., Heshka, N. E., Xin, Q., McMartin, D. W., Peru, K. M., ... & Headley, J. V. (2024). Evaluations of Weathering of Polar and Nonpolar Petroleum Components in a Simulated Freshwater-Oil Spill by Orbitrap and Fourier Transform Ion Cyclotron Resonance Mass Spectrometry. *Energy & Fuels*, 38(8), 6753-6763. <https://doi.org/10.1021/acs.energyfuels.3c04994>
- Bertheussen, A., Simon, S., & Sjöblom, J. (2018). Equilibrium partitioning of naphthenic acid mixture Part 2: crude oil-extracted naphthenic acids. *Energy & Fuels*, 32(9), 9142-9158. <https://doi.org/10.1021/acs.energyfuels.8b01870>
- Brown, T. L., & Rice, J. A. (2000). Effect of experimental parameters on the ESI FT-ICR mass spectrum of fulvic acid. *Analytical Chemistry*, 72(2), 384-390. <https://doi.org/10.1021/ac9902087>
- Derenne, S., & Tu, T. T. N. (2014). Characterizing the molecular structure of organic matter from natural environments: An analytical challenge. *Comptes Rendus Geoscience*, 346(3-4), 53-63. <https://doi.org/10.1016/j.crte.2014.02.005>
- Dittmar, T., Koch, B., Hertkorn, N., & Kattner, G. (2008). A simple and efficient method for the solid-phase extraction of dissolved organic matter (SPE-DOM) from seawater. *Limnology and Oceanography: Methods*, 6(6), 230-235. <https://doi.org/10.4319/lom.2008.6.230>
- Ghassal, B. I. (2019). Reservoir connectivity, water washing and oil to oil correlation: An integrated geochemical and petroleum engineering approach. *SPE Middle East Oil and Gas Show and Conference, MEOS, Proceedings, 2019-March*. <https://doi.org/10.2118/194957-MS>
- Hatcher, P. G., Dria, K. J., Kim, S., & Frazier, S. W. (2001). Modern analytical studies of humic substances. *Soil Science*, 166(11), 770-794. <https://doi.org/10.1097/00010694-200111000-00005>
- Hindle, R., Noestheden, M., Peru, K., & Headley, J. (2013). Quantitative analysis of naphthenic acids in water by liquid chromatography-accurate mass time-of-flight mass spectrometry. *Journal of Chromatography A*, 1286, 166-174. <https://doi.org/10.1016/j.chroma.2013.02.082>
- Jones, D. M., Watson, J. S., Meredith, W., Chen, M., & Bennett, B. (2001). Determination of naphthenic acids in crude oils using nonaqueous ion exchange solid-phase extraction. *Analytical Chemistry*, 73(3), 703-707. <https://doi.org/10.1021/ac000621a>
- Leenheer, Gonsior, M., Zwartjes, M., Cooper, W. J., Song, W., Ishida, K. P., Tseng, L. Y., ... & Schmitt-Kopplin, P. (2011). Molecular characterization of effluent organic matter identified by ultrahigh resolution mass spectrometry. *Water research*, 45(9), 2943-2953. <https://doi.org/10.1016/j.watres.2011.03.016>
- Leenheer, J. A., & Croué, J. P. (2003). Peer reviewed: characterizing aquatic dissolved organic matter. *Environmental science & technology*, 37(1), 18A-26A. <https://doi.org/10.1021/es032333c>
- Leenheer, J. A., & Croué, J. P. (2003). Peer reviewed: characterizing aquatic dissolved organic matter. *Environmental science & technology*, 37(1), 18A-26A. <https://doi.org/10.1021/es032333c>
- Liu, Y., & Kujawinski, E. B. (2015). Chemical composition and potential environmental impacts of water-soluble polar crude oil components inferred from ESI FT-ICR MS. *PLoS one*, 10(9), e0136376. <https://doi.org/10.1371/journal.pone.0136376>
- Maddinelli, G., Bartosek, M., Bonoldi, L., Moghadasi, L., Renna, D., & Moscatelli, D. (2022, October). Parameter Sensitive Inter-Well Tracers to Map Reservoir Conditions. In *Abu Dhabi International Petroleum Exhibition and Conference* (p. D012S140R002). SPE. <https://doi.org/10.2118/211220-MS>
- McCormack, P., Jones, P., Hetheridge, M. J., & Rowland, S. J. (2001). Analysis of oilfield produced waters and production chemicals by electrospray ionisation multi-stage mass spectrometry (ESI-MSn). *Water research*, 35(15), 3567-3578. [https://doi.org/10.1016/S0043-1354\(01\)00070-7](https://doi.org/10.1016/S0043-1354(01)00070-7)
- Osma, L., García, L., Pérez, R., Barbosa, C., Botett, J., Sandoval, J., & Manrique, E. (2019). Benefit-cost and energy efficiency index to support the screening of hybrid cyclic steam stimulation methods. *Energies*, 12(24), 4631. <https://doi.org/10.3390/en12244631>
- Pérez, R. A., Rodríguez, H. A., Rendón, G. J., Plata, B. G., Salinas, L. M., Barbosa, C., ... & Manrique, E. J. (2022, April). Optimizing Production Performance, Energy Efficiency and Carbon Intensity with Preformed Foams in Cyclic Steam Stimulation in a Mature Heavy Oil Field: Pilot Results and Development Plans. In *SPE Improved Oil Recovery Conference* (p. D011S011R002). SPE. <https://doi.org/10.2118/209399-MS>
- Pérez, R. A., Rodríguez, H. A., Romero, J. E., Alvarez, J. S., Hernandez, S., Luque, I., ... & Manrique, E. (2023, June). Incorporating Hybrid Technology of CSS+ Foam in Heavy Oil Field Development Plans: Practical Experiences and Lessons Learned. In *SPE Latin America and Caribbean Petroleum Engineering Conference* (p. D021S009R001). SPE. <https://doi.org/10.2118/213199-MS>
- Pérez, R., Rodríguez, H., Barbosa, C., Manrique, E., García, L., & Rendón, G. (2020, July). Improving CSS Performance with Preformed Foam: Teca-Cocorna Field Case. In *SPE Latin America and Caribbean Petroleum Engineering Conference* (p. D011S002R001). SPE. <https://doi.org/10.2118/199104-MS>
- Pérez-Romero, R. A., García-Duarte, H. A., Osma-Marín, L. Y., Barbosa-Goldstein, C., García-Rodríguez, L. E., Botett-Cervantes, J. A., ... & Manrique-Ventura, E. J. (2020). Downhole heating and hybrid cyclic steam methods: Evaluating technologies from the laboratory to the field. *CT&F-Ciencia, Tecnología y Futuro*, 10(2), 49-60. <https://doi.org/10.29047/01225383.257>
- Reyes, T. G., & Crisosto, J. M. (2016). Characterization of dissolved organic matter in river water by conventional methods and direct sample analysis-time of flight-mass spectrometry. *Journal of Chemistry*, 2016(1), 1537370. <https://doi.org/10.1155/2016/1537370>
- Rowland, S. J., Scarlett, A. G., Jones, D., West, C. E., & Frank, R. A. (2011). Diamonds in the rough: identification of individual naphthenic acids in oil sands process water. *Environmental Science & Technology*, 45(7), 3154-3159. <https://doi.org/10.1021/es103721b>
- Rudzinski, W. E., Oehlers, L., Zhang, Y., & Najera, B. (2002). Tandem mass spectrometric characterization of commercial naphthenic acids and a Maya crude oil. *Energy & Fuels*, 16(5), 1178-1185. <https://doi.org/10.1021/ef020013t>
- Sequera-Dalton, B. M., Gutiérrez, D., Moore, R. G., Mehta, S. A., Ursenbach, M. G., García, H. A., ... & Manrique, E. J. (2024, March). New Insights From an Old Method After History Matching a Newly Designed 1-D Cyclic Steam Stimulation Experiment. In *SPE Canadian Energy Technology Conference* (p. D011S001R001). SPE. <https://doi.org/10.2118/218041-MS>
- Shang, D., Kim, M., Haberl, M., & Legzdins, A. (2013). Development of a rapid liquid chromatography tandem mass spectrometry method for screening of trace naphthenic acids in aqueous environments. *Journal of Chromatography A*, 1278, 98-107. <https://doi.org/10.1016/j.chroma.2012.12.078>

Sleighter, R. L., & Hatcher, P. G. (2007). The application of electrospray ionization coupled to ultrahigh resolution mass spectrometry for the molecular characterization of natural organic matter. *Journal of Mass Spectrometry*, 42(5), 559–574. <https://doi.org/10.1002/jms.1221>

Sørensen, L., Størseth, T. R., Altin, D., Nordtug, T., Faksness, L. G., & Hansen, B. H. (2024). A simple protocol for estimating the acute toxicity of unresolved polar compounds from field-weathered oils. *Toxicology Mechanisms and Methods*, 34(3), 245–255. <https://doi.org/10.1080/15376516.2024.2310003>

Stanford, L.A., Kim, S., Klein, G.C., Smith, D.F., Rodgers, R.P. and Marshall, A. G. (2007). Identification of Water-Soluble Heavy Crude Oil Organic-Acids, Bases, and Neutrals by Electrospray Ionization and Field Desorption Ionization Fourier Transform Ion Cyclotron Resonance Mass Spectrometry. *Environmental Science and Technology*, 41, 2696–2702. <https://doi.org/10.1021/es0624063>

Thomas, K. V., Langford, K., Petersen, K., Smith, A. J., & Tollefsen, K. E. (2009). Effect-directed identification of naphthenic acids as important in vitro xeno-estrogens and anti-androgens in North Sea offshore produced water discharges. *Environmental Science and Technology*, 43(21), 8066–8071. <https://doi.org/10.1021/es9014212>

Venancio, F., Oliveira, A., Silva, S. C., Kina, A. Y., & Mutch, K. (2024, March). Evaluating New Chemical Treatments to Decrease Water Soluble Organic (WSO) Content from Produced Water Discharge. In *SPE Water Lifecycle Management Conference and Exhibition* (p. D011S005R003). SPE. <https://doi.org/10.2118/218979-MS>

Villabona-Estupiñan, S., Rojas-Ruiz, F. A., Pinto-Camargo, J. L., Manrique, E. J., & Orrego-Ruiz, J. A. (2020). Characterization of Petroleum Compounds Adsorbed on Solids by Infrared Spectroscopy and Mass Spectrometry. *Energy & Fuels*, 34(5), 5317–5330. <https://doi.org/10.1021/acs.energyfuels.9b03564>

Wang, G., Xue, Y., Wang, D., Shi, S., Grice, K., & Greenwood, P. F. (2016). Biodegradation and water washing within a series of petroleum reservoirs of the Panyu Oil Field. *Organic Geochemistry*, 96, 65–76. <https://doi.org/10.1016/j.orggeochem.2016.03.009>

Yildiz, H. O., & Morrow, N. R. (1996). Effect of brine composition on recovery of Moutray crude oil by waterflooding. *Journal of Petroleum science and Engineering*, 14(3-4), 159–168. [https://doi.org/10.1016/0920-4105\(95\)00041-0](https://doi.org/10.1016/0920-4105(95)00041-0)

Zheng, F., Shi, Q., Vallverdu, G. S., Giusti, P., & Bouyssièr, B. (2020). Fractionation and characterization of petroleum asphaltene: focus on metalopetroleomics. *Processes*, 8(11), 1504. <https://doi.org/10.3390/pr8111504>

Zito, P., Ghannam, R., Bekins, B. A., & Podgorski, D. C. (2019). Examining the extraction efficiency of petroleum-derived dissolved organic matter in contaminated groundwater plumes. *Groundwater Monitoring & Remediation*, 39(4), 25–31. <https://doi.org/10.1111/gwmmr.12349>

## AUTHORS

### Fernando A. Rojas Ruiz

Affiliation: Ecopetrol S.A. – Instituto Colombiano del Petróleo y energías de la Transición ICPET Piedecuesta, Santander-Colombia.  
ORCID: <https://orcid.org/0000-0002-3566-9498>  
e-mail: fernandoa.rojas@ecopetrol.com.co

### Jorge A. Orrego Ruiz

Affiliation: Ecopetrol S.A. – Instituto Colombiano del Petróleo y energías de la Transición ICPET Piedecuesta, Santander-Colombia.  
ORCID: <https://orcid.org/0000-0002-9087-1074>  
e-mail: jorge.orrego@ecopetrol.com.co

### Angela M. Valencia López

Affiliation: PSL Proanálisis SAS Floridablanca-Santander-Colombia  
ORCID: <https://orcid.org/0000-0003-4690-3742>  
e-mail: angemavalencia@gmail.com

### Romel A. Perez Romero

Affiliation: Petroleum Development Oman, Muscat Oman.  
ORCID: <https://orcid.org/0000-0001-5112-4650>  
e-mail: romelperez83@gmail.com

### Eduardo J. Manrique Ventura

Affiliation: Citation Oil & Gas Corp. Houston, Texas, United States.  
ORCID: <https://orcid.org/0000-0002-0238-8091>  
e-mail: ejmanrique2012@gmail.com

**How to cite:** Rojas-Ruiz et al., (2024). Dissolved Organic Matter (DOM) as Natural Tracking Agent in Cyclic Steam Stimulation with Preformed Foams: A Mature Heavy Oil Field Case. *Ciencia, Tecnología y Futuro - CT&F*. Vol. 14(2), 45 - 57.